LUBRICATION SCIENCE
Lubrication Science 2016; **28**:189–205
Published online 15 October 2015 in Wiley Online Library (wileyonlinelibrary.com). DOI: 10.1002/ls.1325

Analytical model for predicting friction in line contacts

Javier Echávarri Otero*,†, Eduardo de la Guerra Ochoa, Enrique Chacón Tanarro, Andrés Díaz Lantada and Juan M. Munoz-Guijosa

Grupo de Investigación en Ingeniería de Máquinas, Universidad Politécnica de Madrid, Spain

ABSTRACT

This paper presents the development of an analytical model for the prediction of the friction coefficient in line contacts under thermal elastohydrodynamic lubrication (TEHL). A new theoretical equation is deduced for determining the friction coefficient, taking into account the rheology of common lubricants under TEHL. This approach also considers the heat generated and its penetration into the bulk of the contacting solids. Therefore, the increase in temperature and ensuing variations in the operating conditions are determined.

In order to illustrate the use of the new model and verify its accuracy, an experimental stage is performed in a tribological test rig. The predictions of the proposed model are compared with the results obtained in the test rig and other data reported in the literature for diverse lubricants, showing a good agreement in every case.

Received 11 December 2014; Revised 1 September 2015; Accepted 6 September 2015

KEY WORDS: friction coefficient; line contact; thermal elastohydrodynamic lubrication; shear-thinning

NOMENCLATURE

a	Hertz semi-width of the contact (m)
E'	reduced Young's modulus (Pa)
G	shear modulus of the lubricant (Pa)
h_0	minimum film thickness (m)
h_c	central film thickness (m)
h_{Nc}	Newtonian central film thickness (m)
h_{Nct}	Newtonian central film-thickness corrected by thermal effects (m)
I	number of terms of the Gauss-Chebyshev approximation
K	thermal conductivity of a body ($W\,(mK)^{-1}$)
K_l	thermal conductivity of the lubricant ($W\,(mK)^{-1}$)

*Correspondence to: Javier Echávarri Otero, Grupo de Investigación en Ingeniería de Máquinas, Universidad Politécnica de Madrid, Spain.
†E-mail: jechavarri@etsii.upm.es

L_T thermal loading factor
n power-law exponent
p contact pressure (Pa)
p_0 Hertz (maximum) pressure (Pa)
P_E Peclet number
R reduced radius of curvature (m)
SRR slide-to-roll ratio (%)
T temperature of the lubricant (°C)
T_b lubricant bath temperature (°C)
T_{in} lubricant inlet temperature (°C)
T_f flash temperature rise (°C)
u velocity of a surface ($m\,s^{-1}$)
u_m average surface velocity or rolling velocity ($m\,s^{-1}$)
W/L contact load per unit length ($N\,m^{-1}$)
α pressure–viscosity coefficient (Pa^{-1})
β temperature–viscosity coefficient (K^{-1})
$\dot{\gamma}$ shear rate (s^{-1})
ΔT_l average temperature increase due to internal heating of the film (°C)
Δu sliding velocity ($m\,s^{-1}$)
η low-shear viscosity (Pa s)
η_0 low-shear viscosity at ambient pressure (Pa s)
η_G generalised viscosity (Pa s)
μ traction (or friction) coefficient
ρ density ($kg\,m^{-3}$)
σ specific heat ($J\,(kgK)^{-1}$)
τ shear stress (Pa)
φ_T thermal film thickness reduction factor
χ thermal diffusivity ($m^2\,s^{-1}$)

INTRODUCTION

During the last decades, continuous research activity in elastohydrodynamic lubrication has led to progressive understanding of the complex phenomena involved in non-conformal contacts. Starting from the classical studies [1–3] that combined the hydrodynamic effect with the piezoviscous behaviour of the lubricant and deformation of the contacting solids, significant advances have been made from then to the present.[4,5]

Numerous analyses observed that under the severe operating conditions of elastohydrodynamics, the rheology of many common lubricants varies from Newtonian to pseudoplastic.[6,7] Furthermore, it was found that heat generated by friction can produce a local temperature rise, leading to analysis of the thermal effects, and therefore giving rise to the so-called thermal elastohydrodynamic lubrication.[8,9] Many other studies[10–12] contributed to a better understanding of the main factors which influence the behaviour of the lubricant and the quantitative effects of each.

In this way, knowledge of the physical phenomena has been increasingly improving up to a very successful level. This knowledge, combined with the parallel development of the numerical methods,

DOI: 10.1002/ls

allows us to obtain accurate simulations for elastohydrodynamic problems.[13,14] Thus, friction can be predicted, together with the distributions of pressure, film thickness and temperatures of the lubricant and the contacting solids.

Nevertheless, the high accuracy of the numerical methods is frequently in opposition with their complex and tedious application to real case studies. This results in reduced practical use of the simulations, and therefore limiting the possibility of transferring knowledge from research groups to the industry. Among factors that reduce applicability are the requirements of specific software and highly specialised personnel, along with high computational cost and difficult interpretation of the results.

In contrast, this paper presents the development of a predictive model whose application is very simple and suitable for calculation by hand, although the help of a spreadsheet is recommended in order to optimise time and effort. In addition, the fast computation of results makes it useful for pre-modelling purposes, as an initial approach to a complex problem.

The model proposed hereby is based on the theoretical deductions for pseudoplastic lubricants presented in references [15,16] for point contacts. In this paper we focus our attention on line contacts in order to broaden the field of application of the model and cover gears and roller bearings. Although the variation of the contact geometry complicates the analytical process followed in reference [15] to deduce an equation for the friction coefficient, it is possible to derive an easy-to-use formula for line contacts. Subsequently, thermal effects can be added to predict friction in thermal-elastohydrodynamics.

PRESSURE, PIEZOVISCOSITY AND SHEAR-THINNING

Equation (1) shows the pressure distribution and the half-width of dry line contacts, according to Hertz's results,[17] which have shown to be a reasonable approach to behaviour under elastohydrodynamic lubrication. [14]

$$p = p_0\sqrt{1-\frac{x^2}{a^2}};\quad \text{with:}\quad p_0 = \frac{2(W/L)}{\pi a},\quad a = \sqrt{\frac{8(W/L)R}{\pi E'}} \tag{1}$$

The rheology of the lubricant is modelled [18] by means of the Carreau non-Newtonian Equation (2), where the influence of pressure in low-shear viscosity is taken according to Barus law [19,20] and shear rate is simplified to the Couette component [14] in the Hertz region, as customary for analyses of traction.

$$\eta_G = \eta\left[1+\left(\frac{\eta}{G}\dot{\gamma}\right)^2\right]^{\frac{n-1}{2}};\quad \text{with:}\quad \eta = \eta_0 e^{ap}\qquad \dot{\gamma} = \frac{\Delta u}{h_c} \tag{2}$$

Carreau rheological model properly describes the shear-thinning behaviour of many lubricants.[21–23] Carreau Equation (2) introduces two parameters of lubricants, the Carreau's exponent n and the shear modulus G, whose influence in generalised viscosity is outlined in Figure 1.

In Equation (2) film thickness is approached as constant and equal to the central value.[24] Equation (3) gives the Newtonian result h_{Nc} of Hamrock,[25] which, when multiplied by the thermal factor φ_T of

DOI: 10.1002/ls

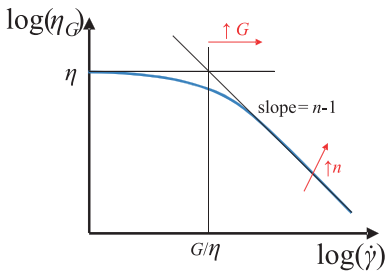

Figure 1. Generalised viscosity versus shear rate for Carreau's model. Influence of the parameters n and G.

Equation (4) provides a corrected value h_{Nct} that considers shear heating effects in the inlet zone.[26,27] Later on, Equation (5) is used to take account of the shear-thinning influence on the film thickness. [28]

$$h_{Nc} = 2.154\alpha^{0.47}(\eta_0 u_m)^{0.692}E'^{0.110}R^{0.308}p_0^{-0.332} \tag{3}$$

$$h_{Nct} = h_{Nc}\cdot\varphi_T; \quad \text{with: } \varphi_T = \frac{1 - 13.2(p_0/E')L_T^{0.42}}{1 + 0.213\left[1 + 2.23\left(\frac{\Delta u}{u_m}\right)^{0.83}\right]L_T^{0.64}}; \quad \text{where: } L_T = \frac{\beta\eta_0 u_m^2}{K_l} \tag{4}$$

$$\frac{h_{Nct}}{h_c} = \left[1 + 0.79\left(\left(1 + \frac{SRR}{100}\right)\frac{u_m\eta_0}{h_{Nct}G}\right)^{\frac{1}{1+0.002SRR}}\right]^{3.6(1-n)^{1.7}} \tag{5}$$

where SRR is defined as the ratio of the sliding velocity Δu to the average (rolling) velocity u_m, expressed as a percentage. Therefore, the central film thickness h_c can be obtained by combining Equations (3), (4) and (5), where empirical formulae (4) and (5) quantify the film thickness reduction due to inlet heating and shear-thinning.

CONTACT TEMPERATURE

According to the studies of Blok, Jaeger and Archard,[29–31] the contact area in dry contacts can be modelled as a concentrated source of heat moving over the surface in order to estimate the rise in temperature during sliding contact. Therefore, it is possible to analytically calculate the so-called 'flash temperature' by applying the laws of energy conservation and heat transfer. Flash temperature is defined as a rise in temperature above the initial bulk temperature of the solids.

A subsequent generalisation of this theory to lubricated contacts assumes that heat is produced through the EHL film and conducted into the contacting solids, without significant heat convected away by the lubricant.[32] The convective term is usually negligible due to the very low EHL film thickness, as reported in references.[33–36] Therefore, the average temperature of the lubricant within the film

DOI: 10.1002/ls

(T) is the sum of the flash temperature rise (T_f), the increase due to internal heating of the film (ΔT_l) and the lubricant inlet temperature (T_{in}),[16]:

$$T = T_f + \Delta T_l + T_{in}. \tag{6}$$

Table I presents a set of formulae for the calculation of average flash temperature for line contacts[29,30]according to three possible scenarios for each body i, distinguished by the Peclet number (P_{Ei}), which takes into account the heat transfer into the bulk of the contacting solids.[32]

As shown in Equation (7), the Peclet number can be computed for each body i, taking into account the half-width of the contact a, the velocity of each surface u_i and the thermal diffusivity of each body χ_i. The latter depends on the thermal conductivity K_i, the density ρ_i and the specific heat σ_i. In this analysis, the thermal properties of the contacting bodies are considered approximately independent of temperature,[32] as their variations for common materials and usual working conditions are very limited.[37]

$$P_{Ei} = \frac{u_i a}{2\chi_i}; \text{ where: } \chi_i = \frac{K_i}{\rho_i \sigma_i} \tag{7}$$

The true flash temperature rise T_f can be calculated[32] using Equation (8), taking into account that all heat generated is divided between the contacting bodies. Thus, T_{fi} ($i = 1, 2$) represents the average flash temperature for each contact body i, calculated as if all the heat generated were conducted to it, using the formulae presented in Table I.

$$\frac{1}{T_f} = \frac{1}{T_{f1}} + \frac{1}{T_{f2}} \tag{8}$$

If one body is stationary the Peclet number for this body is equal to zero. Therefore, according to the first formula from Table I, the average flash temperature for this body tends to infinity. Then, Equation (8) gives a true flash temperature rise equal to the average flash temperature of the other body. On the other hand, when both Peclet numbers are null (both contacting bodies stationary) the true flash temperature rise is equal to zero because there is not heat generation.

A heat balance equation in the lubricant is performed with a method similar to the process presented in reference, [35] applied to the case of line contact. In this way, the following expression is

Table I. Average flash temperature according to the operating scenarios of a solid i (line contact).

Peclet number	Situation considered	Heat penetration	Average flash temperature
$P_{Ei} < 0.1$	Steady state conduction	High	$T_{fi} = 0.318 \frac{\mu (W/L) \Delta u}{K_i P_{Ei}} \left(-2.303 P_{Ei} \log_{10} 2 P_{Ei} + 1.616 P_{Ei}\right)$
$0.1 < P_{Ei} < 5$	Slowly moving heat source	Medium	$T_{fi} = 0.159 \frac{\mu (W/L) \Delta u}{K_i P_{Ei}} \cdot \left(0.423 + 2.663 \cdot P_{Ei} - 0.649 \cdot P_{Ei}^2 + 0.062 \cdot P_{Ei}^3\right)$
$P_{Ei} > 5$	Fast moving heat source	Low	$T_{fi} = 0.376 \frac{\mu (W/L) \Delta u}{K_i P_{Ei}^{1/2}}$

DOI: 10.1002/ls

attained for the average increase in the temperature of the lubricant due to internal heating of the film (ΔT_l).

$$\Delta T_l = \frac{\mu(W/L)\Delta u h_c}{16 a K_l} \tag{9}$$

Thermal conductivity of the lubricant (K_l) can be approached as constant and equal to its value at bath temperature, because of the low variations with temperature reported in reference [32] for most mineral and synthetic lubricants.

Finally, the inlet temperature (T_{in}) and the lubricant bath temperature (T_b) can be related by comparing the expressions for thermal and isothermal film thicknesses (Equations (3) and (4)), obtaining Equation (10). The inlet temperature can be estimated [16] from this equation since the viscosity–temperature relationship is generally known for the lubricant.

$$[\alpha(T_{in})]^{0.47} \cdot [\eta_0(T_{in})]^{0.692} = \varphi_T \cdot [\alpha(T_b)]^{0.47} \cdot [\eta_0(T_b)]^{0.692} \tag{10}$$

It is worth noting that this simplified procedure for calculating temperature does not provide values for temperature distribution. However, the average contact temperature can be estimated with reasonable accuracy. [16]

TRACTION COEFFICIENT

In Couette flow [14] the shear stress can be calculated using the following expression:

$$\tau = \eta_G \dot{\gamma} \tag{11}$$

Taking into account the non-Newtonian model proposed by Carreau, the generalised viscosity Equation (2) is used, and therefore, the following expression (12) is deduced for the friction coefficient by integrating the shear stress in the contact area and dividing by the load.

$$\mu = \frac{2}{\pi} \frac{\eta_0 \Delta u}{h_c a p_0} \int_{-a}^{a} e^{\alpha p_0 \sqrt{1-\left(\frac{x}{a}\right)^2}} \left(1 + \left[\frac{\eta_0 \Delta u}{G h_c} e^{\alpha p_0 \sqrt{1-\left(\frac{x}{a}\right)^2}} \right]^2 \right)^{\frac{n-1}{2}} dx \tag{12}$$

An analytical integration by parts can be performed when the Newtonian shear stress is substantially greater than the parameter G in most of the contact area.[15] In this way, Equation (13) is attained.

$$\mu = \left(\frac{\eta_0 \Delta u}{h_c} \right)^n G^{1-n} \left(\frac{2}{\pi p_0} \left[\frac{x}{a} e^{n\alpha p_0 \sqrt{1-\left(\frac{x}{a}\right)^2}} \right]_{-a}^{a} + \frac{2n\alpha}{\pi} \int_{-a}^{a} \frac{1}{a} \left(\frac{x}{a}\right)^2 \frac{e^{n\alpha p_0 \sqrt{1-\left(\frac{x}{a}\right)^2}}}{\sqrt{1-\left(\frac{x}{a}\right)^2}} dx \right) \tag{13}$$

The process is followed by a variable substitution $X = x/a$, and thus a new integral is found, which allows the use of the Gauss–Chebyshev quadrature for approximating the value of the integral to a finite series. This method can be formulated, in a general way, for a function $f(X)$ as follows:[38]

DOI: 10.1002/ls

$$\int_{-1}^{1} \frac{f(X)}{\sqrt{1-X^2}} dX \approx \frac{\pi}{I} \sum_{i=1}^{I} f(Y_i); \quad \text{where: } Y_i = \cos\left(\frac{2i-1}{2I}\pi\right). \tag{14}$$

In this way, if we take $f(X) = X^2 e^{n\alpha p_0 \sqrt{1-X^2}}$, a new expression (15) can be deduced for the friction coefficient, where *Quad(I)* denotes the Gauss–Chebyshev approximation with I terms, given by Equation (15).

$$\mu = \left(\frac{\eta_0 \Delta u}{h_c}\right)^n G^{1-n} \left[\frac{4}{\pi p_0} + \frac{2n\alpha}{\pi} Quad(I)\right]; \text{ with: } Quad(I) \tag{15}$$

$$= \frac{\pi}{I} \sum_{i=1}^{I} \cos^2\left(\frac{2i-1}{2I}\pi\right) e^{n\alpha p_0 \sqrt{1-\cos^2\left(\frac{2i-1}{2I}\pi\right)}}$$

Table II presents the expressions obtained for the friction coefficient by retaining different number of terms in the series of the Equation (15). The corresponding formulae for the Newtonian case can be easily deduced from Table II by making $n=1$. It is worth noting that the results obtained with four and five terms have been discarded, because they involve more tedious expressions than the case of six terms, whereas accuracy is expected to increase with the number of terms.

In order to find out the accuracy of the Gauss–Chebyshev approximation for different number of terms in the series, it is compared to the results of the numerical solution of the integral term of Equation (13). For this purpose, an interval of values for the group '$n{\cdot}\alpha{\cdot}p_0$' is selected from 2 to 12, which covers typical reference values of lubricants and Hertz pressures.[14] Figure 2(a) depicts the results, where a good accuracy for the analytical approximation with six terms can be observed, with a maximum error of 3% for values of the group '$n{\cdot}\alpha{\cdot}p_0$' under 10. Nevertheless, the deviation becomes higher in other approaches with less terms, namely $I=1$, $I=2$ or $I=3$. Therefore, Equation (16) is selected for computing the friction coefficient.

$$\mu = \left(\eta_0 \frac{\Delta U}{h_c}\right)^n G^{1-n} \left[\frac{4}{\pi p_0} + \frac{n\alpha}{3}\left(1+\frac{\sqrt{3}}{2}\right) e^{n\alpha p_0 \sqrt{\frac{1}{2}-\frac{\sqrt{3}}{4}}} + \frac{n\alpha}{3} e^{n\alpha p_0 \frac{\sqrt{2}}{2}} + \frac{n\alpha}{3}\left(1-\frac{\sqrt{3}}{2}\right) e^{n\alpha p_0 \sqrt{\frac{1}{2}+\frac{\sqrt{3}}{4}}}\right] \tag{16}$$

As observed in Figure 2(b), the error increases for the highest values of the group '$n{\cdot}\alpha{\cdot}p_0$'. Therefore, accuracy could be significantly reduced for unusually high values of '$n{\cdot}\alpha{\cdot}p_0$', i.e. in case of

Table II. Friction coefficient formulae obtained for different number of terms in the series of the Equation (15).

Case	Friction coefficient formula
$I=1$	$\mu = \left(\eta_0 \frac{\Delta U}{h_c}\right)^n G^{1-n} \left[\frac{4}{\pi p_0}\right]$
$I=2$	$\mu = \left(\eta_0 \frac{\Delta U}{h_c}\right)^n G^{1-n} \left[\frac{4}{\pi p_0} + n\alpha e^{n\alpha p_0 \frac{\sqrt{2}}{2}}\right]$
$I=3$	$\mu = \left(\eta_0 \frac{\Delta U}{h_c}\right)^n G^{1-n} \left[\frac{4}{\pi p_0} + n\alpha e^{\frac{n\alpha p_0}{2}}\right]$
$I=6$	$\mu = \left(\eta_0 \frac{\Delta U}{h_c}\right)^n G^{1-n} \left[\frac{4}{\pi p_0} + \frac{n\alpha}{3}\left(1+\frac{\sqrt{3}}{2}\right) e^{n\alpha p_0 \sqrt{\frac{1}{2}-\frac{\sqrt{3}}{4}}} + \frac{n\alpha}{3} e^{n\alpha p_0 \frac{\sqrt{2}}{2}} + \frac{n\alpha}{3}\left(1-\frac{\sqrt{3}}{2}\right) e^{n\alpha p_0 \sqrt{\frac{1}{2}+\frac{\sqrt{3}}{4}}}\right]$

DOI: 10.1002/ls

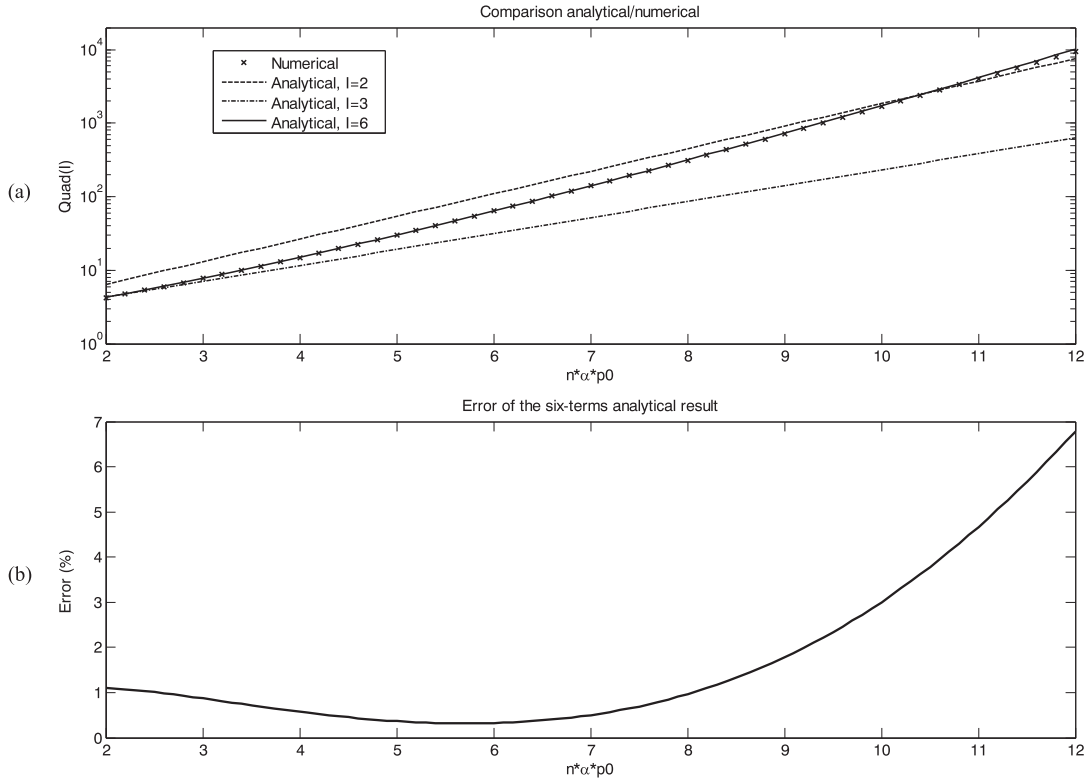

Figure 2. (a) Comparison between the numerical solution and the analytical results for different number of terms used in *Quad(I)*. Note that for $I = 1$ the series in Equation (15) is identically zero; (b) error for the analytical solution with six terms.

extreme pressures, together with lubricants with very high viscosity–pressure coefficient and behaviour close to the Newtonian approach.

METHODOLOGY

The calculation process is similar to that presented in reference,[16] adapted to line contacts through modifications in the equations of Hertzian pressure (1), Newtonian film thickness (3), temperature rise (9, 10 and expressions in Table I) and the new friction coefficient equation developed (16).

In summary, the procedure begins by applying the Hamrock's film thickness equation (3) for the Newtonian and isothermal approach. Later on, thermal effects and shear-thinning are considered through formulae (4) and (5). Once the film thickness is known, the result of Equation (4) can be used to determine whether thermal effects are significant, in line with references[39] and[40] i.e. when thermal factor φ_T is close to one, the regime, can be considered approximately isothermal, and the friction coefficient calculation is facilitated because viscous properties of the lubricant can be introduced at

DOI: 10.1002/ls

bath temperature in expression (16). Otherwise, an iterative process is required for determining the friction coefficient because the viscous properties of the lubricant used in the expression (16) depend on the temperature, which in turn, varies with the friction coefficient.

Therefore, in the non-isothermal case, starting from a hypothesis on the average contact temperature of the lubricant T, the viscous properties are evaluated at this temperature, and the friction coefficient is computed with Equation (16). Then, the temperature is calculated using expressions of Table I, together with Equations (8), (9) and (10). This iterative cycle is repeated until convergence of the initial hypothesis and the calculated value of temperature. Once this process is finished both the friction coefficient and contact temperature are determined.

EXPERIMENTATION

The theoretical results are compared with those given by experimental measurements of the traction (or friction) coefficient, performed on the MPR tribological equipment developed by PCS-Instruments (www.pcs-instruments.com), shown in Figure 3. This equipment is comprised of a set of three rings with the same diameter (54 mm) positioned apart, with a smaller diameter (12 mm) roller located in the middle, in line contact with all the rings. The set of the three rings and roller are driven by independent motors, therefore allowing different combinations of velocity and slide-to-roll ratio. A lubrication system ensures appropriate lubrication of the contact, and an electric cartridge heater is used to adjust the temperature of the lubricant. A loading arm can apply load on the top ring while the lower rings remain fixed. Due to the contact symmetric configuration, the force on each lower ring is equal in magnitude to that applied by the top one. Figure 3 shows the detailed geometry of the roller: the rolling

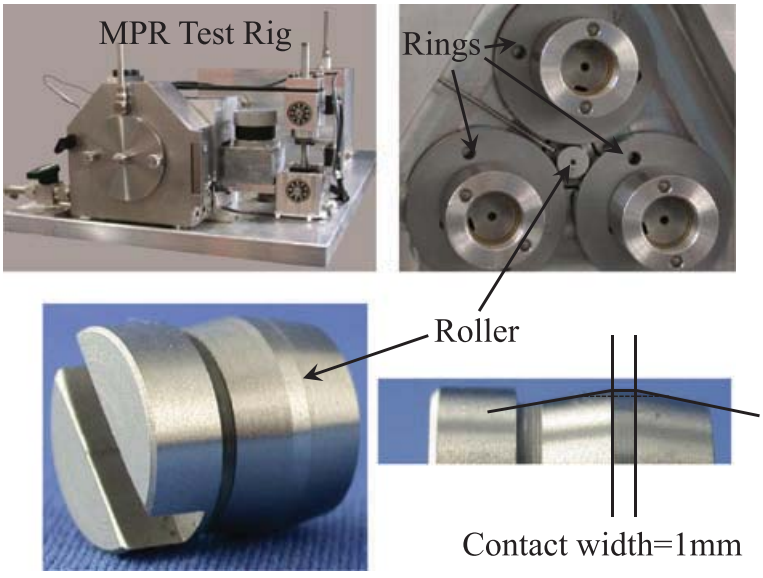

Figure 3. Overview of the MPR and detail of the test zone. Contact width of the roller.

DOI: 10.1002/ls

track has a contact width of 1 mm, with symmetrical chamfers on both sides in order to avoid stress peaks on the edges.

The lubricant chosen is a polyalphaolefin base lubricant PAO-6, whose pseudoplastic behaviour has been reported in references,[15,41] in line with other PAOs.[6,14,28] The physical properties of this fluid were measured in the laboratory and are shown in Table III, giving a temperature–viscosity coefficient of $0.033\,K^{-1}$. The parameters n and G of Carreau's model and the thermal conductivity at 80°C are approximately: [15] $n = 0.81$, $G = 0.1$ MPa and $K_l = 0.15\,W\,(mK)^{-1}$.

Both the properties of the PAO-6 and the operating conditions used in the experiments lead to a range of '$n{\cdot}\alpha{\cdot}p_0$' where the intrinsic error of the friction coefficient formula is under 3%, according to Figure 2(b). The contact material for the rings and the rollers is 16MnCr5 case carburised steel, which presents a Young's modulus of 210 GPa, a Poisson's ratio of 0.3, a thermal conductivity of $41\,W\,(mK)^{-1}$ and a thermal diffusivity of $0.12\,cm^2\,s^{-1}$ approximately. Highly polished rings and rollers are used (RMS roughness lower than 15 nm) in order to ensure EHL conditions for traction calculations, according to references.[42–45] Testing conditions selected are as follows: bath temperature (T_b) of 80°C, average velocities (u_m) of 1.5 and $2\,m\,s^{-1}$, loads of $100\,N\,mm^{-1}$ and $150\,N\,mm^{-1}$, and slide-to-roll ratios from 0 to 190%.

RESULTS AND DISCUSSION

Detailed application of the new model to the PAO-6

According to the methodology explained in 'Methodology', the process begins using Hamrock's formula for film thickness and its ensuing modifications for thermal effects and shear-thinning. Figure 4 shows the calculations of film thickness as a function of the slide-to-roll ratio, at a bath temperature of 80°C, for different average velocities and loads. The results are compared with those of Hamrock's equation, also depicted in Figure 4.

Then, the iterative calculation process is used to determine the average contact temperatures, the results of which are shown in Figure 5. It can be observed that the temperatures found are significantly high, mainly for the highest loads and velocities. Table IV presents an example of the simple iterative calculation, performed until the convergence of the contact temperature, starting from a hypothesis of 100°C. It corresponds to an average velocity of $2\,m\,s^{-1}$, $100\,N\,mm^{-1}$ load, bath temperature of 80°C and SRR = 190%.

Although not required within the calculation process, an intermediate result of interest derived from the model is the shear stress profile in the contact half-width. Figure 6 compares the shear stress in the isothermal and thermal cases for SRRs of 50 and 150%, loads of 100 and $150\,N\,mm^{-1}$, average

Table III. Physical properties of the polyalphaolefin PAO-6.

T (°C)	η_0 (mPa s)	α (GPa^{-1})
30	37.95	12.3
40	25.00	11.5
60	12.57	10.1
80	7.36	9.0
100	4.78	8.2

DOI: 10.1002/ls

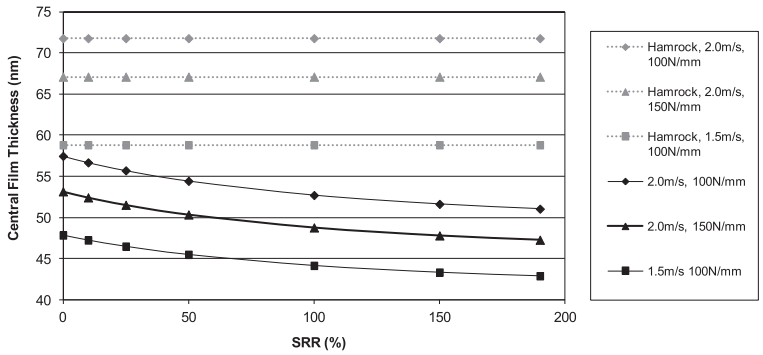

Figure 4. Examples of film thickness calculation for the PAO-6, at $T_b = 80°C$. The horizontal lines represent the results obtained using Equation (3).

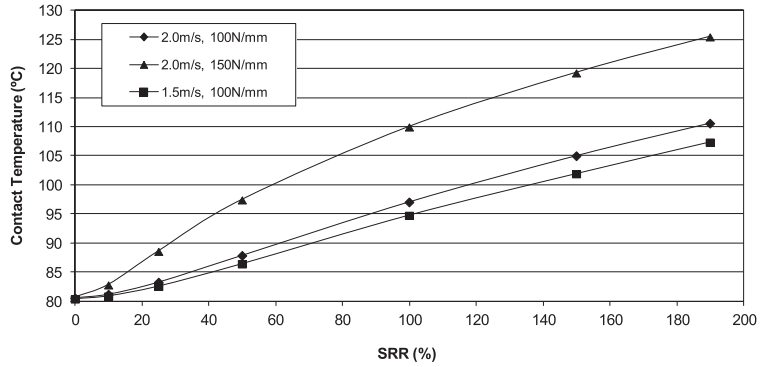

Figure 5. Examples of temperature calculation for the PAO-6, at $T_b = 80°C$.

Table IV. Iterative process for calculating the contact temperature and the friction coefficient.

Iteration	Hypothesis T (°C)	Friction coefficient, μ	Calculated T (°C)	Deviation (°C)
First	100.00	0.0514	132.34	32.34
Second	110.00	0.0304	111.69	1.69
Third	110.50	0.0296	110.91	0.41
Fourth	110.70	0.0293	110.61	−0.09
Fifth	110.65	0.0294	110.68	0.03

velocity of $2\,m\,s^{-1}$ and bath temperature of 80°C. The increase of SRR or load leads to moving the results away from the isothermal behaviour.

Finally, Figure 7 compares the experimental friction coefficient with the corresponding predictions attained using the isothermal and thermal analytical approaches for a bath temperature of 80°C, under loads of 100 and $150\,N\,mm^{-1}$, and average velocities of 1.5 and $2\,m\,s^{-1}$. It is worth noting that each traction coefficient value in Figure 7 corresponds to an average value of several series of 28

DOI: 10.1002/ls

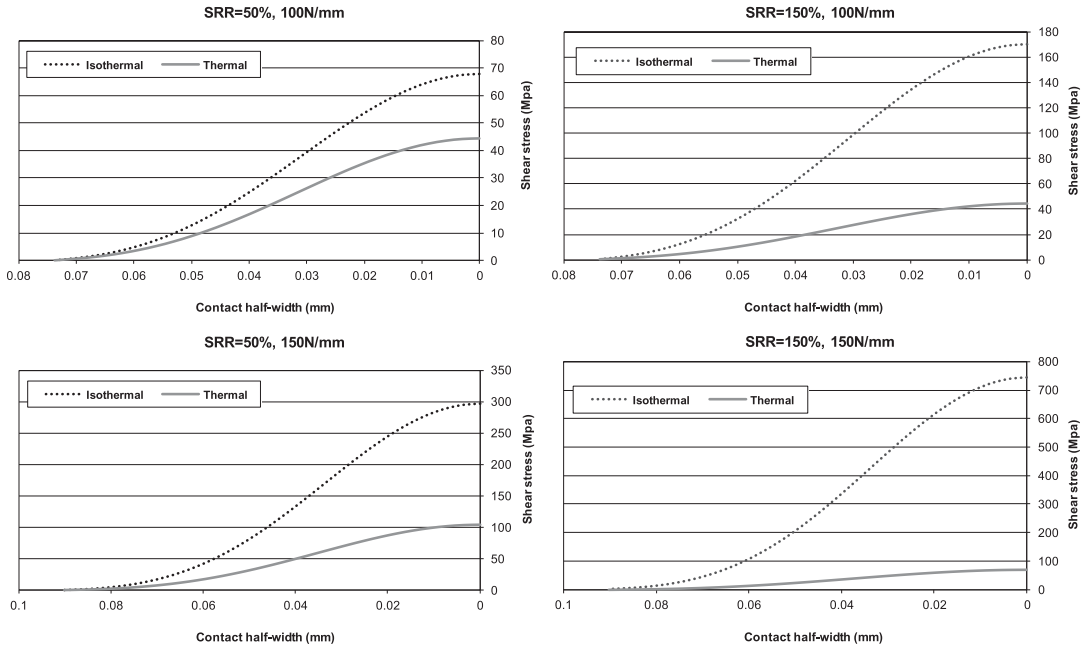

Figure 6. Calculating shear stress in the contact area. Examples for $2\,\mathrm{m\,s^{-1}}$ and $T_b = 80°\mathrm{C}$.

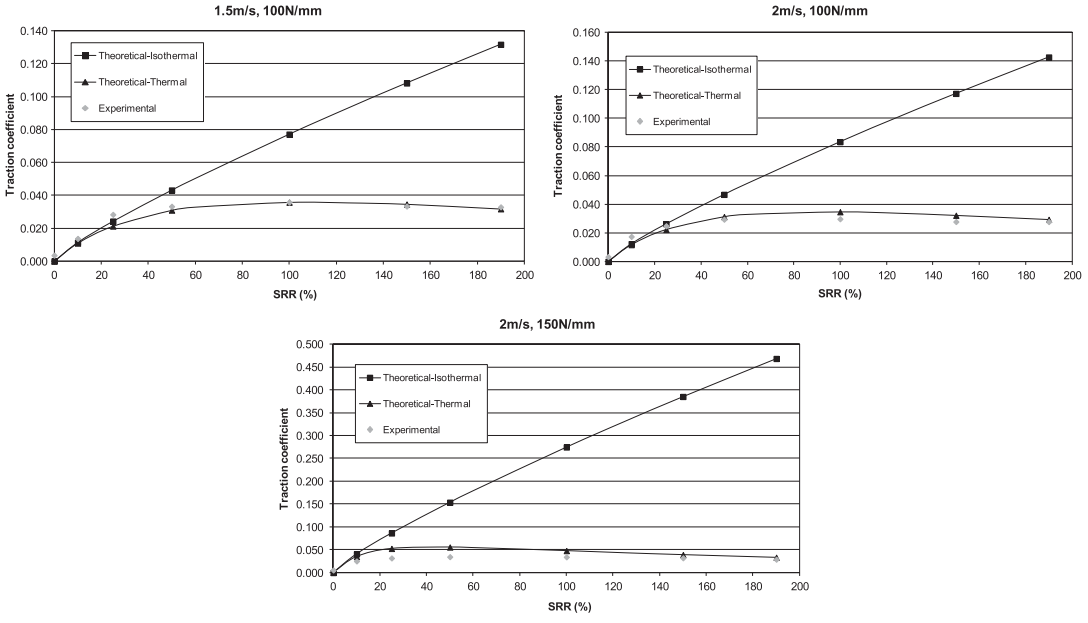

Figure 7. Comparison of analytical and experimental results for the friction coefficient of a PAO-6 using both isothermal and thermal approaches for different loads, average velocities and SRRs.

DOI: 10.1002/ls

measurements under the same testing conditions in the MPR. Control steps are used during the test to check repeatability. After finishing the test with a set of rings and a roller, the same test is repeated using new samples. By the way of example, Figure 8 presents results of different repetitions, along with their means and deviations, which show a reasonably good repeatability.

As observed in Figure 7, the isothermal model overestimates the friction, whereas the thermal one more accurately predicts the friction coefficient. These results are in line with the contact temperatures shown in Figure 5, which demonstrates a non-isothermal behaviour of the contact except for low SRRs.

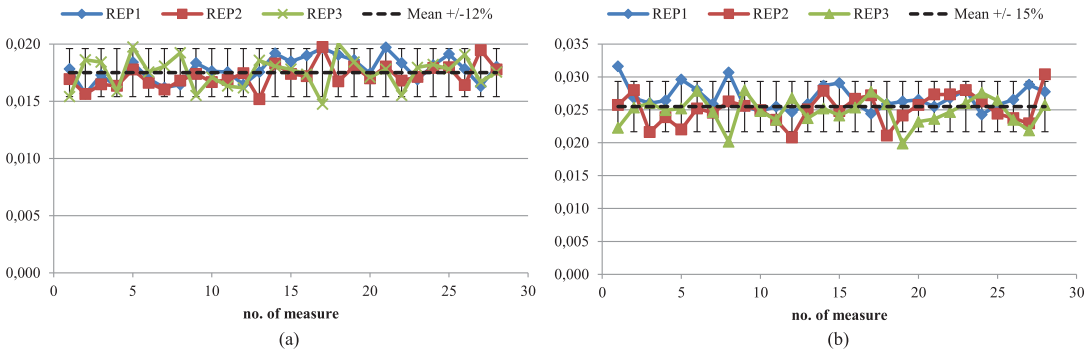

Figure 8. Repeatability analysis of the tests: (a) $u_m = 2\,\mathrm{m\,s^{-1}}$, $SRR = 10\%$, $W/L = 100\,\mathrm{N\,mm^{-1}}$; (b) $u_m = 2\,\mathrm{m\,s^{-1}}$, $SRR = 10\%$, $W/L = 150\,\mathrm{N\,mm^{-1}}$.

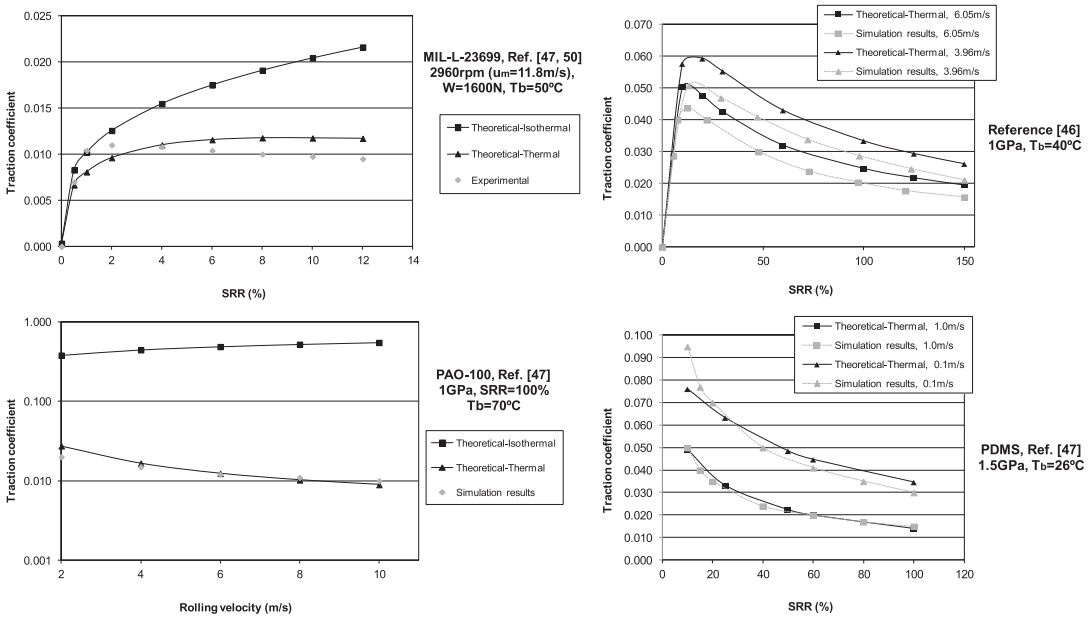

Figure 9. Comparison of the new analytical model with the results published in references [46,47] for different lubricants and operating conditions.

DOI: 10.1002/ls

The effect of increasingly heating with the rise of *SRR* is also observed in Figure 6 because shear stress results differ more and more from the isothermal result.

Application of the model to other lubricants

As for applying the model described in this paper to other lubricants, the main difficulty found is the limited information available about the rheology of the lubricants under the extreme operating conditions of pressure, temperature and slide velocity, which are typical in EHL. Nevertheless, for lubricants whose rheological properties are known, a reasonably accurate prediction of the friction coefficient is attained.

By way of example, Figure 9 shows a comparison between the traction coefficient data published for both Newtonian and pseudoplastic lubricants [46,47] and predictions of the model presented in this paper. The rheological properties of the lubricants used in this study are taken from references,[14,21,46–51] as summarised in Table V. The parameter '$n{\cdot}\alpha{\cdot}p_0$' has been calculated in all the cases to ensure an intrinsic error in the friction coefficient formula under 3%, according to Figure 2(b). In every case, the friction coefficient results obtained for the new model show good correlation with the experimental data and the simulation results presented by other authors, with an average deviation of 12%. Significant thermal effects can be appreciated by comparing isothermal and thermal approaches, although in some cases the isothermal result is omitted for clarity purposes. Furthermore, taking into account the cases where film thickness and temperature predictions are available,[13,49] Table VI suggests a good agreement of the new model with the results published.

Table V. Rheological properties of other lubricants.[14,21,46–51] Average values of n and G were fitted through experimental results in references.[14,21,47]

Lubricant	T_b (°C)	η_0 (mPa s)	α (GPa^{-1})	n	G (MPa)
MIL-L-23699	50	15.5	9.6	0.3	4.0
PAO-100	70	181.0	10.9	0.625	1.5
Newtonian	40	40.0	8.9	1.0	∞
PDMS	26	491.0	16.42	0.33	0.13

Table VI. Comparison of dimensionless film thickness and contact temperature of the new model with other published data. Results for a Hertz maximum pressure of 1 GPa.

Reference		Kumar & Khonsari		Lee & Hsu		This paper	
SRR (%)	u_m (m s^{-1})	h_0R/a^2	T (°C)	h_0R/a^2	T (°C)	h_0R/a^2	T (°C)
10	3.96	0.0895	60.29	0.0853	61.31	0.0720	58.87
10	6.05	0.1140	68.37	0.1084	69.76	0,0896	67.02
20	3.96	0.0858	78.63	0.0815	80.00	0.0708	75.11
20	6.05	0.1090	88.85	0.1045	90.09	0.0872	85.48
30	3.96	0.0824	91.52	0.0783	93.09	0.0700	86.81
30	6.05	0.1049	102.66	0.1006	104.46	0.0851	98.39

DOI: 10.1002/ls

CONCLUSIONS

Bearing in mind the good results of the analytical thermal elastohydrodynamic model presented previously for point contacts, an analogue method has been proposed in this paper for line contacts. For this purpose, a new formula has been developed for predicting the friction coefficient. The results of the new analytical model have been validated experimentally and with the predictions of other authors.

Once the accuracy has been verified, it is important to note that a major advantage of the new model is its simple and analytical formulation, leading to a method suitable for calculation by hand. Although the implementation of the process in a spreadsheet facilitates its use, neither specific software nor specialised personnel are required.

Therefore, we hope that the new model will be useful from a practical standpoint, due to its easy, quick and reliable predictions of friction, film thickness and contact temperature in thermal elastohydrodynamic line contacts.

ACKNOWLEDGEMENTS

This work was carried out as a part of the Research Project DPI2013-48348-C2-2-R, financed by the Spanish Ministry of Economy and Competitiveness. We would also like to thank the Lubricants Laboratory of Repsol.

REFERENCES

1. Grubin AN. Fundamentals of the hydrodynamic theory of lubrication of heavily loaded cylindrical surfaces. in *Proceedings of Symposium on Investigation of the Contact of Machine Components*, Kh. F. Ketova (ed.), Book no. 30. Moscow, Russia, 1949.
2. Dowson D, Higginson GR. A numerical solution to the elastohydrodynamic problem. *Journal of Mechanical Engineering Science* 1959; **1**(1):6–15.
3. Hamrock BJ, Dowson D. Isothermal elastohydrodynamic lubrication of point contacts. Part III—fully flooded results. *Journal of Lubrication Technology* 1977; **99**:264–276.
4. Dowson D. *History of Tribology,* Longman, London, (2nd edn), 1998.
5. Echavarri J, De la Guerra E, Chacón E. Tribology: an historical overview of the relation between theory and application. in *A Bridge Between Conceptual Frameworks, Sciences, Society and Technology Studies*, R Pisano (ed), Springer, Dordrecht 2014.
6. Bair S. A Reynolds–Ellis equation for line contacts with shear-thinning. *Tribology International* 2006; **39**:310–316.
7. Bair S, Winer WO. Some observations in high pressure rheology of lubricants. Trans. ASME, *Journal of Lubrication Technology.* 1982; **104**:382–386.
8. Kumar P, Anuradha P, Khonsari MM. Some important aspects of thermal elastohydrodynamic lubrication. *Proceedings IMechE Part C: Journal of Mechanical Engineering Science* 2010; **224**:2588–2598.
9. Hsiao HS, and Hamrock BJ. A complete solution for thermal-elastohydrodynamic lubrication of line contacts using circular non-Newtonian fluid model. *J. TWM., ASME* paper 91-Trib-24, 1992.
10. Johnson KL, Tevaarwerk JL. Shear behaviour of elastohydrodynamic oil films. *Proceedings of the Royal Society of London Series A*, 1977; **356**:215–236.
11. Höglund E. Influence of lubricant properties on elastohydrodynamic lubrication. *Wear* 1999; **232**:176–184.
12. Stähl J, Jacobson BO. A non-Newtonian model based on limiting shear stress and slip planes—parametric studies. *Tribology International* 2003; **36**:801–806.
13. Kumar P, Khonsari MM. Combined effects of shear thinning and viscous heating on EHL characteristics of rolling/sliding line contacts. *Journal of Tribology* 2008; **130**:1–13.
14. Bair S. *High Pressure Rheology for Quantitative Elastohydrodynamics. Tribology and Interface Engineering Series*, vol. **54**. Elsevier, Amsterdam 2007.
15. Lafont P, Echávarri J, Sánchez-Peñuela JB, Muñoz JL, Díaz A, Munoz-Guijosa JM, Lorenzo H, Leal P, Muñoz J. Models for predicting friction coefficient and parameters with influence in elastohydrodynamic lubrication. *Proceedings IMechE Part J: Journal of Engineering Tribology* 2009; **223**(J7):949–958.

DOI: 10.1002/ls

16. Echávarri J, Lafont P, Chacón E, de la Guerra E, Díaz A, Munoz-Guijosa JM, Muñoz JL. Analytical model for predicting friction coefficient in point contacts with thermal elastohydrodynamic lubrication. *Proceedings IMechE Part J: Journal of Engineering Tribology* 2011; **225**:181–191.
17. Hertz H *On the contact of elastic solids*. In Miscellaneous papers. Eds. H. Hertz. D.E. Jones and G.A. Schort, 1896, *pp. 146–162* (Macmillan, London).
18. Carreau PJ. Rheological equations from molecular network theories. *Transactions. Society of Rheology* 1972; **16**(1):99–127.
19. Barus C, Isotherms, isopiestics and isometrics relative to viscosity. *American Journal of Science* 1893; **45**:87–96.
20. Vergne P, Bair S, Classical EHL Versus Quantitative EHL: A perspective part I—real viscosity-pressure dependence and the viscosity-pressure coefficient for predicting film thickness. *Tribology Letters* 2014; **54**(1):1–12.
21. Chapkov AD, Bair S, Cann P, Lubrecht AA. Film thickness in point contacts under generalized Newtonian EHL conditions: numerical and experimental analysis. *Tribology International* 2007; **40**:1474–1478.
22. Liu Y, Wang QJ, Bair S, Vergne P. A quantitative solution for the full shear-thinning EHL point contact problem including traction. *Tribology Letters* 2007; **28**(2):171–181.
23. Jang JY, Khonsari MM, Bair S. On the elastohydrodynamic analysis of shear-thinning fluids. *Proceedings of Royal Society A* 2007; **463**:3271–3290.
24. Carli M, Sharif KJ, Ciulli E, Evans HP, Snidle RW. Thermal point contact EHL analysis of rolling/sliding contacts with experimental comparison showing anomalous film shapes. *Tribology International* 2009; **42**(4):517–525.
25. Hamrock BJ. *Fundamentals of Fluid Film Lubrication*. McGraw-Hill, New York 1994.
26. Cheng HS. Calculations of elastohydrodynamic film thickness in high speed rolling and sliding contacts, *Mechanical Technology, Inc*. Technical Report, MTI-67TR24, 1967.
27. Gupta PK, Cheng HS, Forster NH, Schrand JB. Viscoelastic effects in MIL-L-7808-type lubricant. I: Analytical formulation. *Tribology Transactions* 1992; **35**(2):269–274.
28. Bair S. Shear thinning correction for rolling/sliding elastohydrodynamic film thickness. *Proceedings IMechE Part J: Journal of Engineering Tribology* 2005; **219**:69–74.
29. Blok H. *Theoretical Study of Temperature Rise at Surfaces of Actual Contact Under Oiliness Lubricating Conditions. General Discussion on Lubrication*, vol. **2**. Inst. Mech. Engrs: London, 1937, 222–235.
30. Jaeger JC. Moving sources of heat and the temperature at sliding contacts. *Proceedings Royal Society of New South Wales* 1943; **76**:203–224.
31. Archard JF. The temperature of rubbing surfaces. *Wear* 1958/59; **2**:438–455.
32. Stachowiak GW, Batchelor AW. *Engineering Tribology*, Elsevier Butterworth-Heinemann, Amsterdam 2005.
33. Trachman ED. The rheological effects on friction in elastohydrodynamic lubrication. Ph.D. Thesis, Northwestern Uni versity, 1971.
34. Wang KL and Cheng HS. Thermal elastohydrodynamic lubrication of spur gears. NASA Contractor Report 3241.
35. Olver AV, Spikes HA. Prediction of traction in elastohydrodynamic lubrication, *Proceedings IMechE Part J: Journal of Engineering Tribology* 1998; **212**:321–332.
36. Gohar R, Rahnejat H. *Fundamentals of Tribology*, Imperial College Press, London 2008.
37. Incropera FP, DeWitt DP, Bergman TL, Lavine AS. *Fundamentals of Heat and Mass Transfer*, John Wiley & Sons, New York 2007.
38. Abramowitz M, Stegun IA. *Handbook of Mathematical Functions*, Dover Publications, Michigan 1972.
39. Jubault I, Molimard J, Lubrecht AA, Mansot JL, Vergne P. In situ pressure and film thickness measurements in rolling/sliding lubricated point contacts. *Tribology Letters* 2003; **15**(4):421–429.
40. Habchi W, Vergne P, Bair S, Andersson O, Eyheramendy D, Morales-Espejel GE. Influence of pressure and temperature dependence of thermal properties of a lubricant on the behavior of circular TEHD contacts. *Tribology International* 2010; **43**:1842–1850.
41. Hernández Battez A, Viesca JL, González R, García A, Reddyhoff T, Higuera-Garrido A. Effect of shear rate, temperature, and particle concentration on the rheological properties of ZnO and ZrO_2 nanofluids. *Tribology Transactions* 2014; **57**:489–495.
42. P Vergne. Super low traction under EHD and mixed lubrication regimes. in *Superlubricity*, A Erdemir, Martin JM (eds), Elsevier BV, Amsterdam 2007, 429–445.
43. Castro J, Seabra J. Coefficient of friction in mixed film lubrication: gears versus twin-discs. *Proceedings IMechE, Part J: Journal of Engineering Tribology* 2007; **221**:399–411.
44. Zhu D, Hu Y. A computer program package for the prediction of EHL and mixed lubrication characteristics, friction, subsurface stresses and flash temperatures based on measured 3-D surface roughness. *STLE Tribolibology Transactions* 2001; **44** (3):383–309.

DOI: 10.1002/ls

45. Brandão A, Seabra J, Castro J. Surface initiated tooth flank damage Part I: Numerical model. *Wear* 2010; **268**:1–12.
46. Masjedi M, Khonsari MM. Theoretical and experimental investigation of traction coefficient in line-contact EHL of rough surfaces. *Tribology International* 2014; **70**:179–189.
47. Kumar P, Khonsari MM. Traction in EHL line contacts using free-volume pressure–viscosity relationship with thermal and shear-thinning effects. *Journal of Tribology* 2009; **131**:1–8.
48. Sadeghi F, Sui PC. Thermal elastohydrodynamic lubrication of rolling/sliding contacts. *Journal of Tribology* 1990; **112**(2):189–195.
49. Lee R-T, H Chao-Ho. A fast method for the analysis of thermal-elastohydrodynamic lubrication of rolling/sliding line contacts. *Wear* 1993; **166**:107–117.
50. Kannel JJ, Dow TA. The relation between pressure and temperature in rolling–sliding EHD contact. *ASLE Transactions* 1980; **23**(3):262–268.
51. Anuradha P, Kumar P. Effect of lubricant selection on EHL performance of involute spur gears. *Tribology International* 2012; **50**:82–90.

DOI: 10.1002/ls